

## Geometry of dynamically available empty space is the key to near-arrest dynamics

Aonghus Lawlor,<sup>1,\*</sup> Paolo De Gregorio,<sup>1</sup> Phil Bradley,<sup>1</sup> Mauro Sellitto,<sup>2</sup> and Kenneth A. Dawson<sup>1</sup>

<sup>1</sup>*Department of Chemistry, University College Dublin, Irish Centre for Colloid Science and Biomaterials, Belfield, Dublin 4, Ireland*

<sup>2</sup>*The Abdus Salam International Centre for Theoretical Physics, Strada Costiera 11, 34100 Trieste, Italy*

(Received 6 October 2004; revised manuscript received 23 May 2005; published 3 August 2005)

We study several examples of kinetically constrained lattice models using dynamically accessible volume as an order parameter. Thereby we identify two distinct regimes exhibiting dynamical slowing, with a sharp threshold between them. These regimes are identified both by a new response function in dynamically available volume, as well as directly in the dynamics. Results for the self-diffusion constant in terms of the connected hole density are presented, and some evidence is given for scaling in the limit of dynamical arrest.

DOI: [10.1103/PhysRevE.72.021401](https://doi.org/10.1103/PhysRevE.72.021401)

PACS number(s): 61.43.Fs, 64.60.Ak

In nature, molecules, particles or other elements of a nearly arrested system may sometimes stop moving without any accompanying sharp change in the thermodynamic quantities. Such systems have not crystallized, the free energy has not been minimized, and there is no obvious order parameter for the “transition.” This phenomenon of precipitous, and apparently collective, loss of motion has been named “dynamical arrest” [1–5], or jamming [6–8]. It is involved in the “glass transition” [9] and even, apparently, gellation [10,11]. In the field of glassification especially, very significant advances have been made in developing our understanding [12,13]. In the scientific community there is an emerging opinion that the many modes by which complex condensed states are formed are all aspects of the process of dynamical arrest.

We have sought a fundamental theoretical approach to dynamical arrest [2,3] based on a physical order parameter to describe the vicinity of dynamical arrest, keeping in mind the potential to make direct contact with experiment. In particular, the advent of new experiments [14,15], and new experimental methods [16–18] being developed in colloidal and soft matter science, opens up the possibility to directly connect observation of particle configurations and their fluctuations to suitably framed theoretical concepts. We have identified dynamically available volume (DAV) [2], the ensemble of physical space available to particle dynamics, as a possible order parameter. Its use has been illustrated in a recent study of certain lattice models that exhibit dynamical arrest [2,3,19] and has been considered in models of granular matter [6].

In this paper, we highlight a new insight that for the simple model systems we explore, and possibly more generally in nature, the geometry of available empty space of a nearly arrested system has a profound impact on the nature of the relaxation processes and the accompanying laws governing the onset of arrest. We propose that the onset of arrest involves two qualitatively different regimes, both of which appear to exhibit a degree of universality and scaling not previously appreciated. Our observations are valid for a variety of lattice types, and in both two and three spatial dimensions.

The models we study include kinetically constrained lattice models introduced by Kob and Andersen [20] in which particles may move to an adjacent empty site (a hole) if surrounded by  $c$  or fewer neighbors, and if the movement is reversible according to these same rules. Vacancies are empty sites into which no adjacent particle can move. A dynamical arrest transition occurs as a function of increasing particle density, system size, spatial dimensionality  $d$ , and constraints  $c$ .

At moderate densities a particle that moves into a hole typically generates a new hole that may be used for a subsequent motion. By such sequential motions, all particles in the system may be moved beginning with such a (“connected”) hole. At high density many (“disconnected”) holes are caged by a continuous boundary of particles that cannot be broken by particle rearrangements inside the boundary (e.g., in the square-lattice KA model the boundary has at least a double row of particles of rectangular shape). Each particle on this boundary is blocked because it cages, and is caged by, its neighbors. In our previous work we deemed disconnected holes irrelevant for the long length and time scale transport coefficients, and the connected holes (of density  $\nu_c$ ) become the natural order parameter [2]. Subsequently [3] it has become apparent that, asymptotically close to final arrest (in the lattice models, for  $\rho=1$ ) this is equivalent, via the relation  $\nu_c=1/\xi^d$ , to relating the transport coefficients to the bootstrap length  $\xi$  [21,22].

Connected and disconnected hole densities can be estimated by numerical simulation, or by theoretical approaches [3]—in some two-dimensional models they can be calculated exactly [19]. The total hole density  $\nu_t$  is a sum of the connected  $\nu_c$  and disconnected  $\nu_d$  hole densities, and  $\nu_c$  is plotted for  $c=d=2$  KA in Fig. 1 ( $c=d=3$  KA in the inset). Although the results shown here for the connected hole densities, or equivalently, the bootstrap length  $\xi^d=1/\nu_c$  correspond to bootstrap simulations for system sizes beyond any previously computed, it is important to note that they remain far too small [3,19] to be described by simple (exact) asymptotic approximations [23].

The connected hole density is the order parameter of the dynamical system and determines the transport coefficients. The response of the dynamical system to creation of a hole may be calculated from the derivative (essentially a response function for hole creation)  $\chi_c=\partial\nu_c/\partial\nu_t$ , plotted as a function

\*Electronic address: [aonghus@fiachra.ucd.ie](mailto:aonghus@fiachra.ucd.ie)

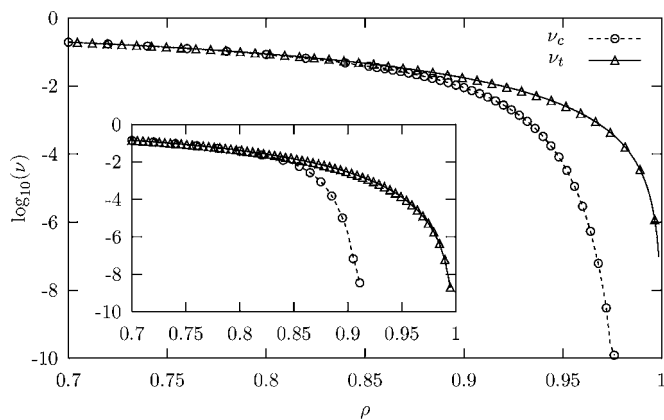


FIG. 1. Total ( $\nu_t$ ) and connected ( $\nu_c$ ) hole density for the 2D and 3D (inset) Kob-Andersen model-largest length corresponding to  $\xi = 10^5$  for 2D and  $\xi = 10^3$  for 3D.

of density for the  $c=d=2$  KA model in Fig. 2. The result is striking—we find a threshold (“transition”) density below which new holes automatically become connected (and therefore contribute to diffusion) and above which nearly all holes are trapped within extended cages.

To the low density (“unstable”) side of the transition a new hole is typically close to an existing connected hole, and therefore likely also to be connected. More holes lead to further mobility, and the system is termed unstable. However, this mechanism also implies that dynamical connectedness, formerly defined only in relation to phase space (the possibility to move all particles from a given initial condition), is strongly associated with geometrical aspects of a network of connected holes in this regime.

To the high density (“metastable”) side of the transition, creation of a new hole typically leads to a rattler, or disconnected hole due to caging. Existing connected holes are now dispersed sufficiently far apart that they provide no assistance to a new hole.

The small peak in  $\chi_c$  (at  $\nu_c^*$ ) is considered the onset of this transformation of phase space, and the peak of the second derivative,  $\eta_c = \partial^2 \nu_c / \partial \nu_t^2$ , an effective threshold at which the system may be deemed to have made a “transition” in dy-

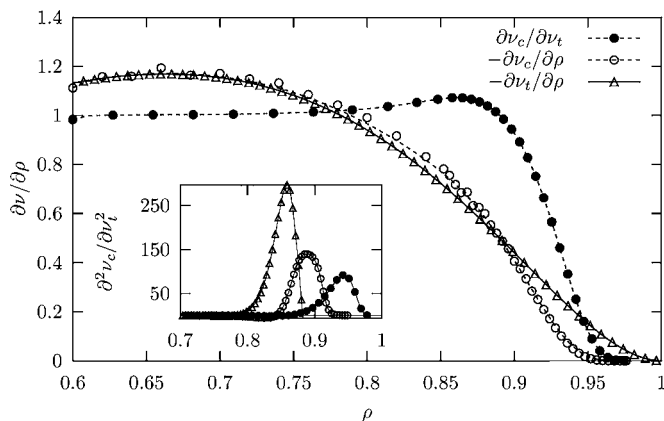


FIG. 2.  $\chi_c = \partial \nu_c / \partial \nu_t$  for  $d=2$  KA model. Also shown are  $-\partial \nu_c / \partial \rho$  ( $\circ$ ) and  $-\partial \nu_t / \partial \rho$  ( $\triangle$ ). The inset shows  $\eta_c = \partial^2 \nu_c / \partial \nu_t^2$  for cubic KA  $c=3$  ( $\circ$ ), fcc KA  $c=6$  ( $\triangle$ ), and KA  $c=d=2$  ( $\bullet$ ).

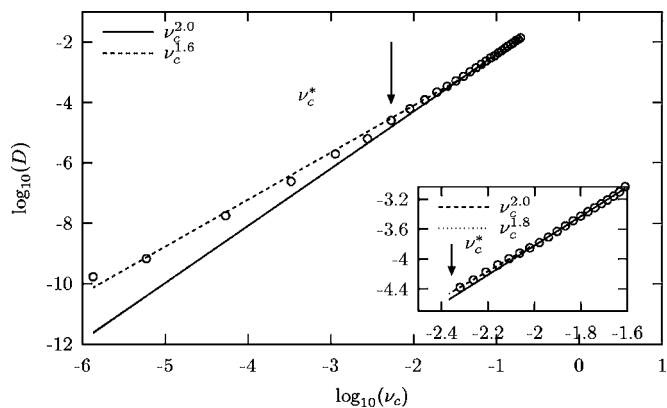


FIG. 3. Diffusion constants for 2D and 3D (inset) for KA.

namics (see inset to Fig. 2). In that inset we show that a similar reorganization of phase space is observable in models with different sets of kinetic constraints, symmetry of lattice, and spatial dimensionality. It should be emphasized that it has so far been difficult to quantitatively relate this restructuring of phase space, and the change in dynamical processes, to simple static concepts of connectedness of vacancy and hole networks, though attempts continue [24]. On the contrary, for each of the different models described in this inset there are quite different spatially connected networks, while the dynamical phenomenon is quite general. Note carefully that the connected hole density contains information on the potential temporal evolution of the system. We now consider the important step in understanding the geometrical aspects involves the concept of response functions. These are defined one level removed from the specific rules of the model itself that capture the spatio-temporal connectedness of phase space. This approach is expected to be more appropriate also in attempts to generalize to the continuum.

We conclude there are likely two quite distinct dynamically slowed regimes on approach to arrest, possessing qualitatively different spatio-temporal or dynamical relaxation processes, different laws for the diffusion constant, and nonlinear response functions. There is ample anecdotal experimental information for differing dynamical regimes, and possibly differing types of law, but hitherto there has been no clear formulation of the underlying ideas. We are in a position to check this explicitly in the dynamics of these models. Note, however, that the strength of the calculations above are that they are (or may be made) essentially exact, whereas the dynamics calculations are lengthy with more limited reliability. We shall now establish the existence of two different regimes for these models by exploring different aspects of the dynamics.

The mean squared distances traveled by particles  $\langle r(t)^2 \rangle$  are computed as usual [2], and the diffusion constants  $D$  calculated from the long-time diffusivity  $\langle r(t)^2 \rangle = 2dDt$  (see Fig. 3). Having computed the relation between the connected hole density and particle density we may eliminate the latter and plot the diffusion constant in terms of the order parameter,  $\nu_c$ . It is known that the connected hole density fails to reach a simple asymptotic form in any density range accessible to computers [3,19,25–28]. Indeed, in the regimes we

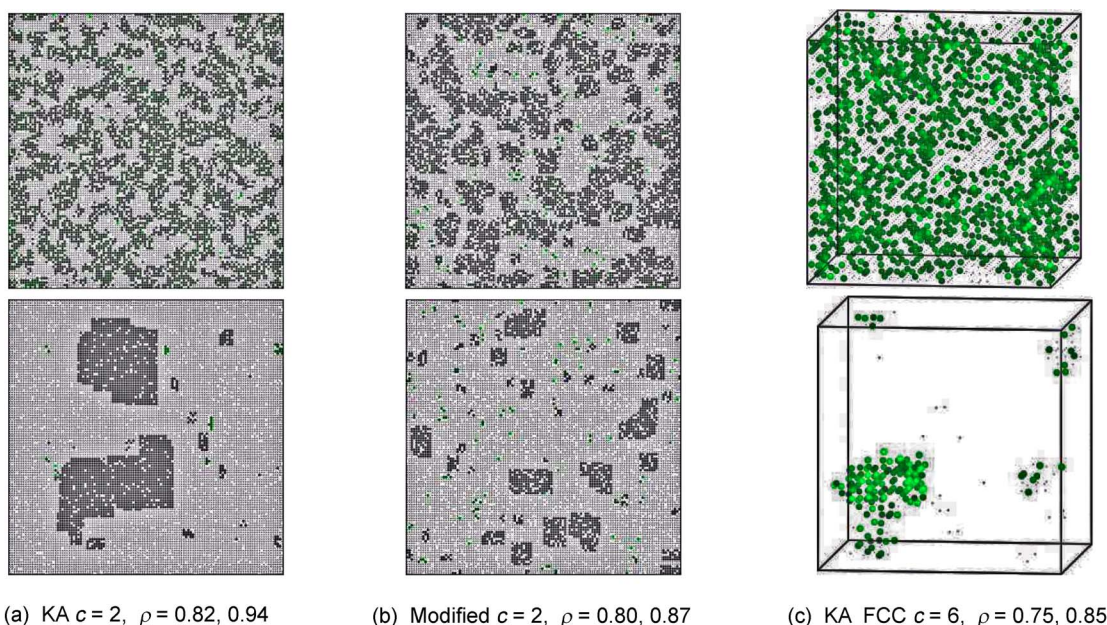


FIG. 4. (Color online) Sample configurations of simulations of different models in the unstable regimes (upper panels) and metastable regimes (lower panels). We show only the particles that have moved after some time. The patterns in the upper panels develop almost immediately, while those on the bottom are essentially unchanged after many millions of MCS. These give a pictorial representation of how dynamically accessible volume is delocalized in the system, and thereby characterize the nature of the relaxation processes in the two regimes. In the unstable regime spinodal-like waves spread throughout the system, while in the metastable system movement initiates in localized droplets, and spreads slowly from those (rare) seeds.

discuss, there is a difference of several orders of magnitude from the asymptotic form that is usually assumed. Therefore, in writing the diffusion constant in terms of the connected hole density (or dynamical correlation or bootstrap length) it is important to use results that are appropriate to the density regime under consideration.

For moderate density we recover the known [2] quadratic law  $D = \gamma \nu_c^2$ , ( $\gamma$  is a model-dependent effective rate constant) for different models, rules sets, and spatial dimensions. In that regime  $\nu_c$  and  $\rho$  (and therefore  $D$  and  $\rho$ ) are connected by a power law. However, at higher densities, for those models that have been explored beyond the “transition,” there is a sharp change of slope and a new law for the diffusion constant,  $D = \gamma \nu_c^z$  ( $z$  noninteger). In that regime the hole density (and thereby diffusion constant) is connected to particle density via an exponential-like decay, though the detailed form is subtle [3]. In each case we have marked that value of particle density at which the unstable-to-metastable transition takes place based on available volumes. Examples are given for two- and three-dimensional KA models, but similar phenomena are present in several other lattice types, and kinetic constraint sets. For the three-dimensional cubic lattice the crossover is on the edge of the presently accessible length and time scales.

One should not be complacent about quantitative treatment of this high density limit as, for example, expressed in the (effective) exponents  $z$ , which may contain a slowly varying density dependence. The fact that the diffusion constants are derived from some of the longest simulations and large system sizes is no reassurance; the dangers of interpretation associated with the (related) subtle asymptotic phe-

nomena in the bootstrap percolation problem where system sizes far beyond current computation fail to reach asymptotic laws is sufficient warning [3,19,23,29]. Here we will seek to clarify the distinct physical relaxation processes. The true asymptotics may have to wait for developments in dynamics that mirror those that have taken place recently in the bootstrap problem.

Amongst the most striking way to illustrate the consequences in dynamics of the transition described in Fig. 2 is to represent the spatio-temporal processes themselves visually. Thus in Fig. 4 we illustrate qualitatively different dynamics of unstable and metastable regimes from several models using two representative densities on either side of the geometrical transition.

The examples correspond to  $c=d=2$  KA and KA modified and  $c=6$ , fcc KA models (the  $c=2$  KA modified model is identical to the  $c=2$  KA model with the added restriction that when we consider a move, any of the two vacant neighbors of the particle must be second neighbors to each other). In each case the particles which have moved after some time are shown in their initial positions. We have explored many examples, and found the phenomena we describe to be quite general. In the unstable regime motion spreads rapidly in a concerted manner, with ample pathways for configurational relaxation arising from implied networks of connected holes. At higher particle densities, the available volume disconnects (“de-percolates”), leading to the metastable regime. There the pathways are quite different; the motion is much slower and mediated by “droplets” within which connected holes mobilize the particles with the assistance of a network of vacancies. These pictures, illustrating the mechanisms by

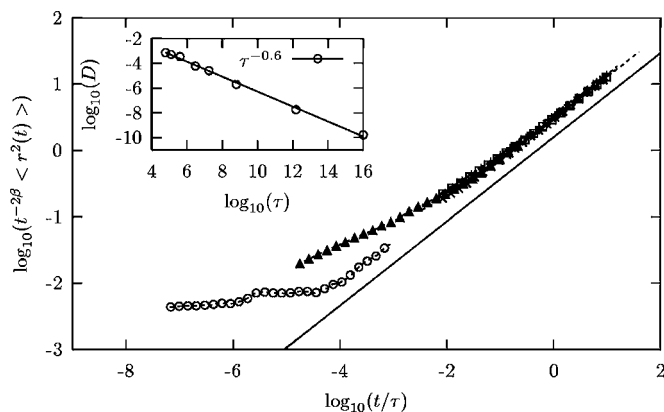


FIG. 5. Scaling of the mean square displacement  $\langle r^2 \rangle = t^{2\beta} f(t/\tau)$  for 2D KA in the metastable regime. The densities are  $\rho=0.850$  ( $\diamond$ ),  $\rho=0.860$  ( $+$ ),  $\rho=0.870$  ( $\square$ ),  $\rho=0.900$  ( $\times$ ),  $\rho=0.930$  ( $\triangle$ ) at  $L=512$  and  $\rho=0.950$  ( $\circ$ ) at  $L=1024$ . In the inset we show the diffusion constant against crossover time.

which dynamically available volume is delocalized and configurational relaxation occurs, are quite consistent with the understanding of the two regimes arising from the susceptibility ( $\chi_c$ ) alone, affirming the value and link between dynamics, and static averages in available volumes, based on bootstrap processes.

We end by noting that the metastable regime appears to exhibit a characteristic time, and a degree of scaling, on approach to true dynamical arrest. Thus, in Fig. 5 we show the scaled curves, and in the inset the equivalent crossover time ( $\tau$ ) at which the system becomes diffusive. The scaling behavior, and the requirement for appropriate short- and long-time behavior, leads us to write  $\langle r^2 \rangle = t^{2\beta} f(t/\tau)$  with  $f(x) \sim \text{const}$  (small  $x$ ) and  $f(x) \sim x^\alpha$  (large  $x$ ). Here  $\beta$  is an exponent reflecting the subergodic nature of the system up to the

crossover time [30]. The two asymptotic behaviors match at the crossover time, leading to  $R^2 = D\tau$ ,  $R^2 = \tau^{2\beta}$ , and therefore  $D \sim \tau^{2\beta-1}$ . For large density the connected hole density is written in terms of the bootstrap length, and therefore we finally obtain the law,  $D \sim \nu_c^\mu$  with  $\mu = -(2\beta-1)/\beta d$ . From the cross-over data we estimate the exponent  $\mu=1.7$ , in good agreement with direct measurements, and in accord with recent studies of a similar model, the two-vacancy assisted triangular lattice gas [31]. The uncertainties of using cross-over data are considerably larger than the direct measurement of the exponent from the diffusion constant data above in Fig. 3, but the routes are entirely independent, and therefore valuable in the context of the present uncertainties about finite size dependence. We conclude that it is possible that the cascade of cages and partial cages determining the subergodic behavior provides a set of scalable “traps,” and thereby a collapse of the dynamics data as outlined above.

In summary, we propose the existence of two regimes of near-arrested dynamics with a transition between them driven by the underlying geometry of available volume. The geometrical properties of this empty space are not simple, but are characterized by a new response function. The two regimes possess different relaxation processes, leading to different dependencies of the diffusion constant on density. That change in the diffusion constants could, for some cases, be so dramatic to be mistaken for the dynamical arrest itself. One would expect to be able to observe the geometrical transition in direct imaging experiments, and its consequences via new experimental methods that can probe long-time and long-length-scale dynamics in colloidal and nano-particle science.

The work is supported by MCRN-CT-2003-504712. Conversations with G. Biroli, S. Franz, and C. Toninelli are acknowledged.

- 
- [1] M. Mézard and G. Parisi, *J. Phys.: Condens. Matter* **12**, 6655 (2000).
- [2] A. Lawlor, D. Reagan, G. D. McCullagh, P. De Gregorio, P. Tartaglia, and K. A. Dawson, *Phys. Rev. Lett.* **89**, 245503 (2002).
- [3] P. De Gregorio, A. Lawlor, P. Bradley, and K. A. Dawson, *Phys. Rev. Lett.* **93**, 025501 (2004).
- [4] L. Berthier and J. P. Garrahan, *Phys. Rev. E* **68**, 041201 (2003).
- [5] Y. J. Jung, J. P. Garrahan, and D. Chandler, *Phys. Rev. E* **69**, 061205 (2004).
- [6] A. Mehta and G. C. Barker, *J. Phys.: Condens. Matter* **12**, 6619 (2000).
- [7] A. J. Liu and S. R. Nagel, *Nature (London)* **396**, 21 (1998).
- [8] T. M. Truskett, S. Torquato, and P. G. Debenedetti, *Phys. Rev. E* **62**, 993 (2000).
- [9] W. Götze, in *Freezing and Glass Transition*, edited by J. P. Hansen, D. Levesque, and J. Zinn-Justin (North Holland, Amsterdam, 1991), p. 287.
- [10] K. Dawson, G. Foffi, M. Fuchs, W. Götze, F. Sciortino, M. Sperl, P. Tartaglia, T. Voigtmann, and E. Zaccarelli, *Phys. Rev. E* **63**, 011401 (2001).
- [11] K. A. Dawson, *Curr. Opin. Colloid Interface Sci.* **7**, 218 (2002).
- [12] W. Götze and L. Sjögren, *Rep. Prog. Phys.* **55**, 241 (1992).
- [13] F. H. Stillinger, *Science* **267**, 1935 (1995).
- [14] W. K. Kegel and A. van Blaaderen, *Science* **287**, 290 (2000).
- [15] E. R. Weeks, J. C. Crocker, A. C. Levitt, A. Schofield, and D. A. Weitz, *Science* **287**, 627 (2000).
- [16] F. Scheffold, S. E. Skipetrov, S. Romer, and P. Schurtenberger, *Phys. Rev. E* **63**, 061404 (2001).
- [17] Z. Cheng, J. Zhu, and P. M. Chaikin, *Phys. Rev. E* **65**, 041405 (2002).
- [18] L. Cipelletti, H. Bissig, V. Trappe, P. Ballesta, and S. Mazoyer, *J. Phys.: Condens. Matter* **15**, S257 (2003).
- [19] P. D. Gregorio, A. Lawlor, P. Bradley, and K. A. Dawson, *Proc. Natl. Acad. Sci. U.S.A.* **102**, 5669 (2005).
- [20] W. Kob and H. C. Andersen, *Phys. Rev. E* **48**, 4364 (1993).
- [21] J. Jäckle and A. Krönig, *J. Phys.: Condens. Matter* **6**, 7633 (1994).

- [22] C. Toninelli, G. Biroli, and D. S. Fisher, Phys. Rev. Lett. **92**, 185504 (2004).
- [23] A. Holroyd, Probab. Theory Relat. Fields **125**, 195 (2003).
- [24] A. Lawlor, P. De Gregorio, and K. A. Dawson, unpublished.
- [25] J. Adler and D. Stauffer, J. Phys. A **23**, L1119 (1990).
- [26] J. Adler, Physica A **171**, 453 (1991).
- [27] N. S. Branco and C. J. Silva, Int. J. Mod. Phys. C **10**, 921 (1999).
- [28] D. Kurtsiefer, Int. J. Mod. Phys. C **14**, 529 (2003).
- [29] J. Adler and U. Lev, Braz. J. Phys. **33**, 641 (2003).
- [30] R. Rammal and G. Toulouse, J. Phys. (Paris), Lett. **44**, L13 (1983).
- [31] A. Pan, J. Garrahan, and D. Chandler, e-print cond-mat/0410525.